Electronic Supplementary Material (ESI) for CrystEngComm.

Supporting Information

Enhancing stability of Metal−Organic Framework via ligand modification: scalable synthesis and highly selectivity of CO_2 sorption property

Di-Ming Chen*, Xue-Jing Zhang

Henan Provincial Key Laboratory of Surface & Interface Science, Zhengzhou University of Light Industry, Zhengzhou 450002, P. R. China

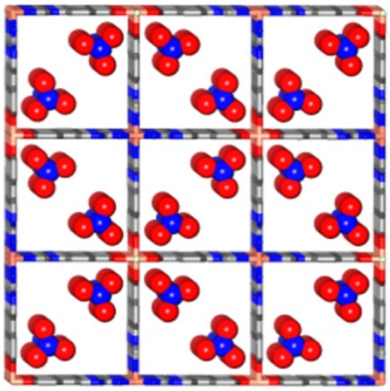

Fig S1. The location of NO_3^- in the framework of **1**.

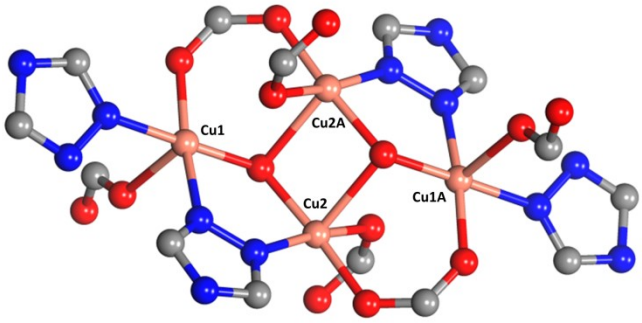

Fig S2. The coordination environment of the Cu^{2+} ions in the tetranuclear copper cluster (Symmetry code A: 1–x, –y, 1–z).

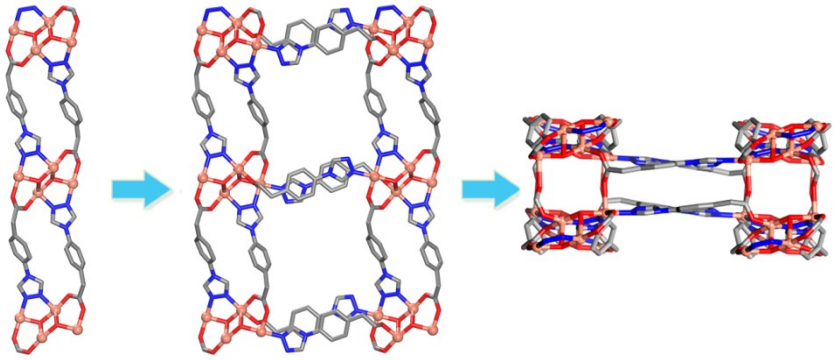

Fig S3. The schematic representation of the formation of the double-walled structure of **2**.

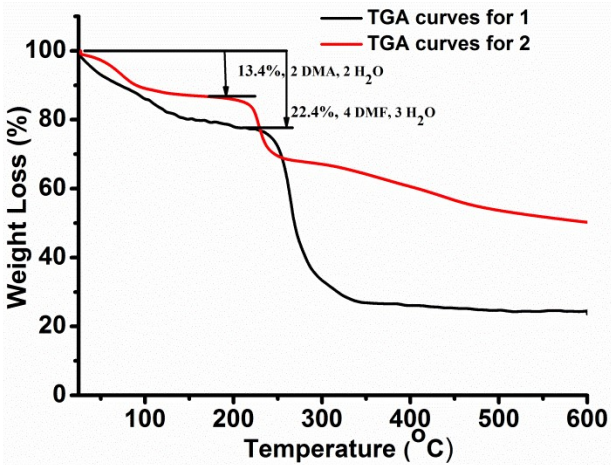

Fig S4. The TG curves for the single-walled **1** and double-walled **2.**

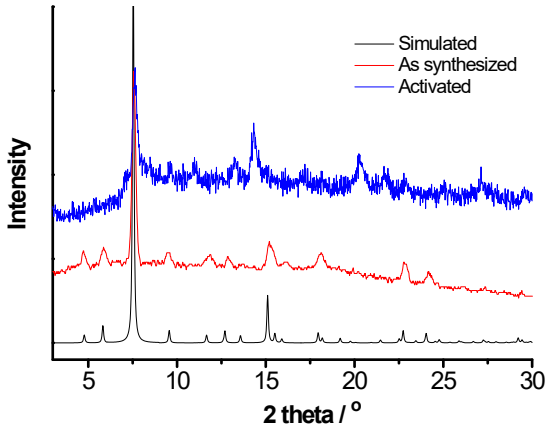

Fig S5. Powder X-ray diffraction (PXRD) patterns of **1**: pattern simulated from single-crystal structure in black, experimental pattern for the as-synthesized sample in red, experimental pattern for the activated sample in blue.

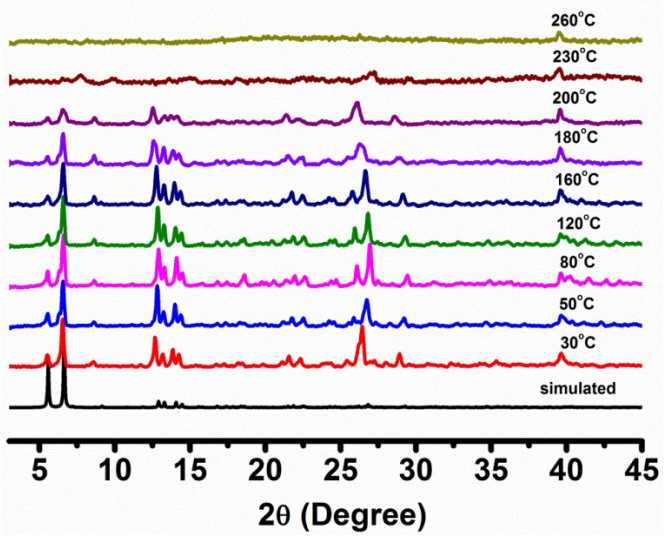

Fig S6. Variable temperature PXRD pattern of double-walled **2**.

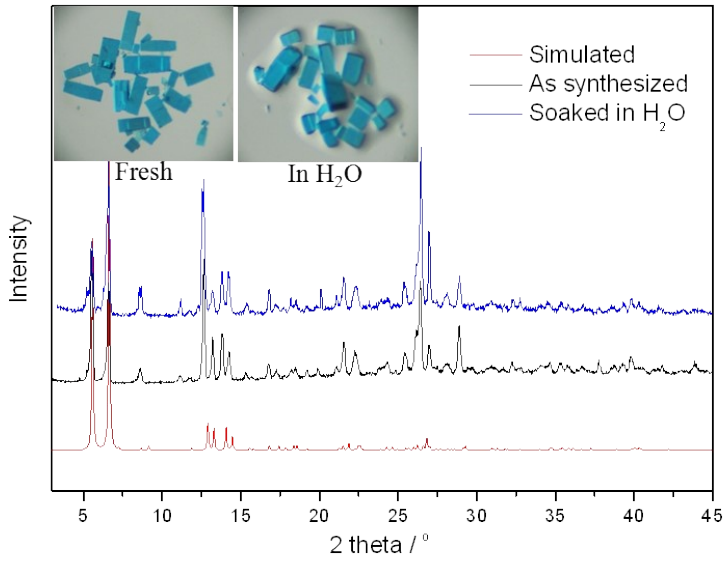

Fig S7. PXRD patterns of **2**: pattern simulated from single-crystal structure in red, experimental pattern for the as-synthesized sample in black, experimental pattern for the sample soaked in H_2O in blue. Insert photos for **2** as synthesized and soaked in H_2O.

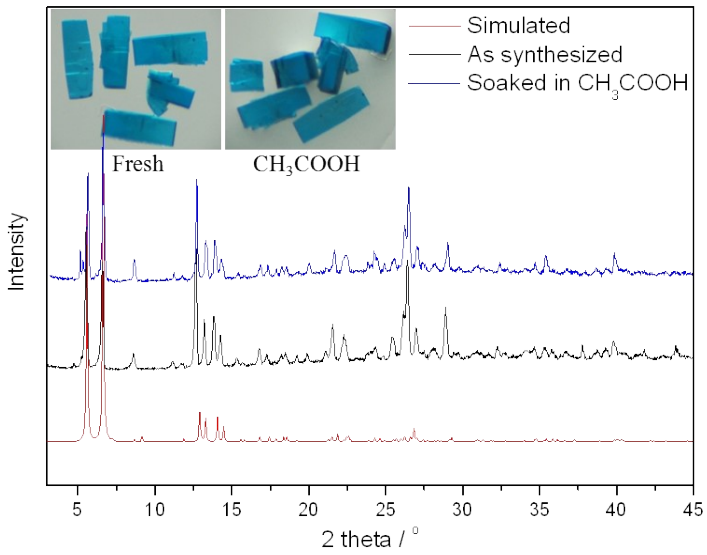

Fig S8. PXRD patterns of **2**: pattern simulated from single-crystal structure in red, experimental pattern for the as-synthesized sample in black, experimental pattern for the sample soaked in CH_3COOH in blue. Insert photos for **2** as synthesized and soaked in CH_3COOH.

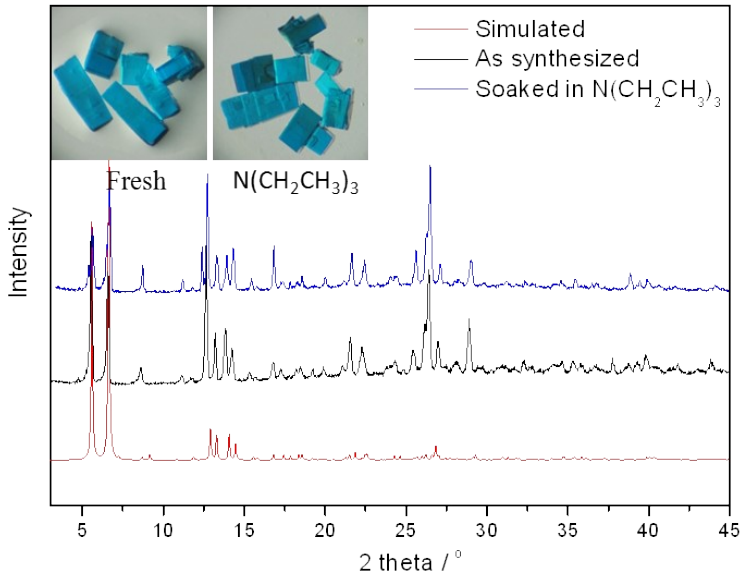

Fig S9. PXRD patterns of **2**: pattern simulated from single-crystal structure in red, experimental pattern for the as-synthesized sample in black, experimental pattern for the sample soaked in $N(CH_2CH_3)_3$ in blue. Insert photos for **2** as synthesized and soaked in $N(CH_2CH_3)_3$.

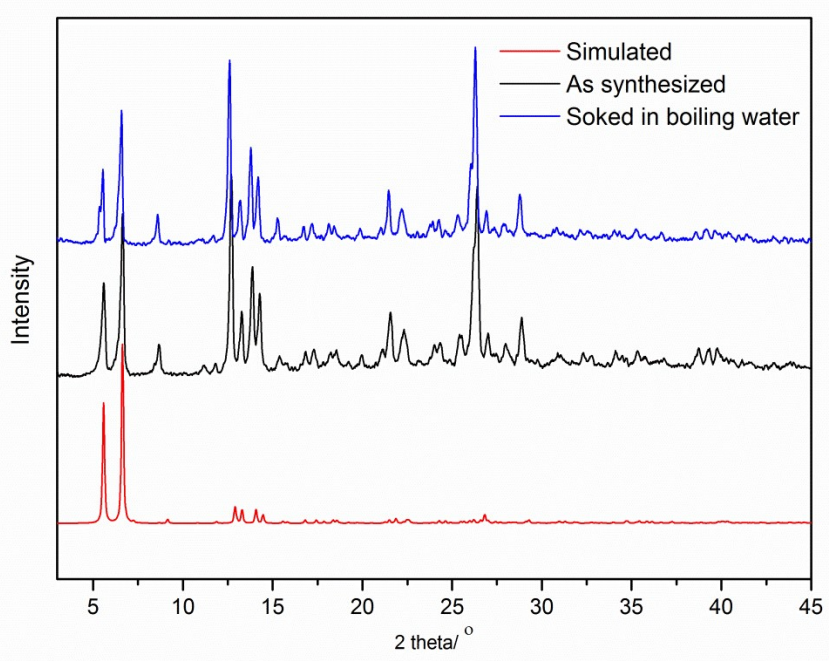

Fig S10. PXRD patterns of **2**: pattern simulated from single-crystal structure in red, experimental pattern for the as-synthesized sample in black, experimental pattern for the sample soaked in boiling water in blue.

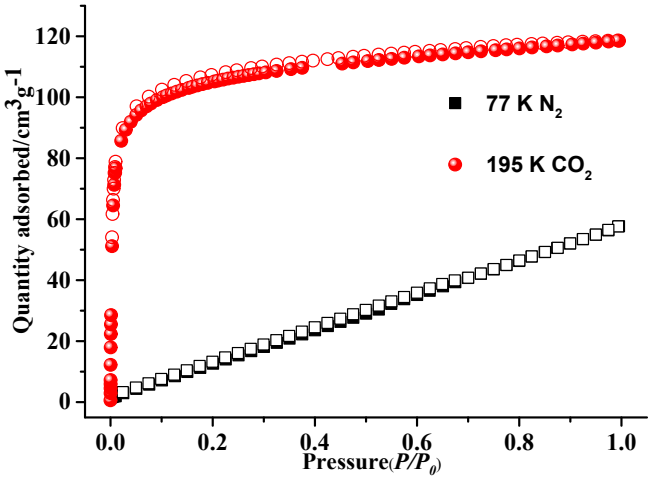

Fig S11. The 195 K CO_2 sorption isotherm and 77 K N_2 sorption isotherm of **2**′.

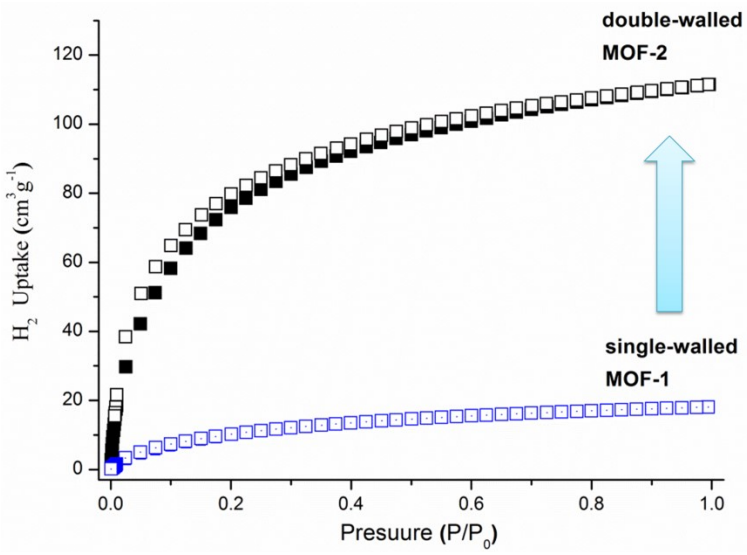

Fig S12. H_2 adsorption isotherms of **1** and **2.**

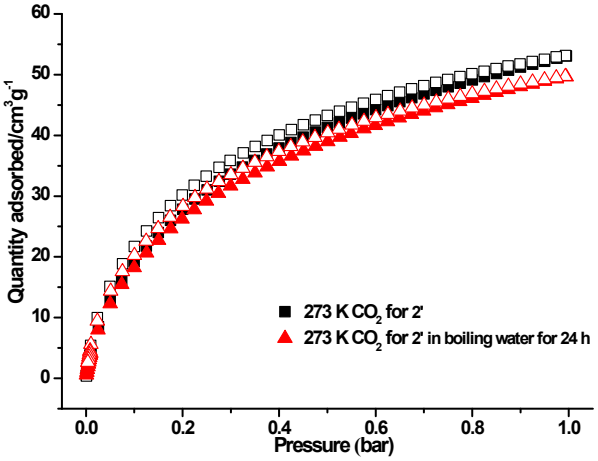

Fig S13. CO_2 sorption isotherms of **2'** and **2'** in boiling water for 24 h.

Calculations of CO_2/CH_4 and CO_2/N_2 selectivities based on IAST

The experimental isotherm data on pure component for CO_2, N_2 and CH_4 were measured at temperatures of 273 and 298 K, which were fitted by single-site-Langmuir–Freundlich model (SSLF):

$$y = \frac{abx^{1-c}}{1+bx^{1-c}}$$

The adsorption selectivities for binary mixtures of CO_2/CH_4 and CO_2/N_2, defined by

$$S_{i/j} = \frac{x_i * y_j}{x_j * y_i}$$

were respectively calculated using the Ideal Adsorption Solution Theory (IAST). Where xi is the mole fraction of component i in the adsorbed phase and yi is the mole fraction of component i in the bulk.

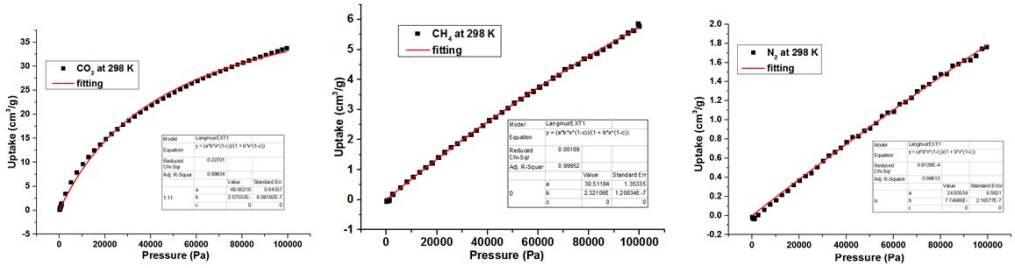

Fig. S14 single site Langmuir–Freundlich fitting for the sorption data of **2'**.

Calculation of sorption heat for CO_2 uptake using Virial model:

$$\ln P = \ln N + 1/T \sum_{i=0}^{m} aiN^i + \sum_{i=0}^{n} biN^i \qquad Q_{st} = -R \sum_{i=0}^{m} aiN^i$$

The above equation was applied to fit the combined CO_2 isotherm data for **2'** at 273 and 298 K, where P is the pressure, N is the adsorbed amount, T is the temperature, ai and bi are virial coefficients, and m and n are the number of coefficients used to describe the isotherms. Q_{st} is the coverage-dependent enthalpy of adsorption and R is the universal gas constant.

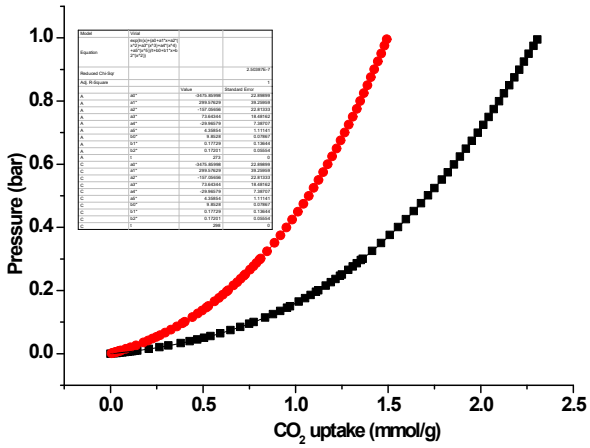

Fig. S15 CO_2 adsorption isotherms for **2'** with fitting by Virial model.

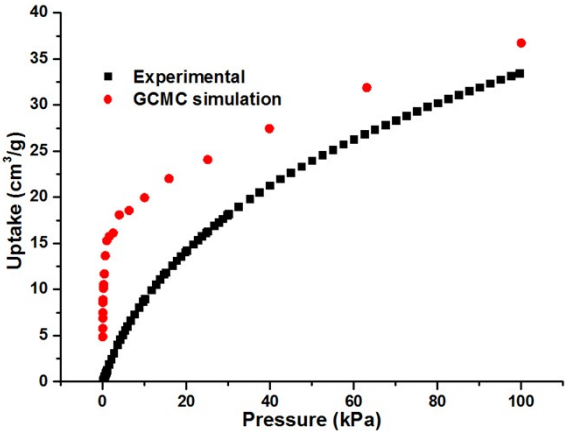

Fig S16. The experimental and simulated sorption isotherms of **2'**.

Table S1. Crystal data and structure refinement.

	1	**2**	**2(after Sorption)**
Empirical formula	$C_{48}H_{58}ClCu_4N_{19}O_{24}$	$C_{48}H_{56}Cu_4N_{18}O_{24}$	$C_{40}H_{32}Cu_4N_{14}O_{18}$
Formula weight	1571.72	1523.25	1250.95
Temperature/K	293(2)	120(2)	298(3)
Crystal system	tetragonal	orthorhombic	orthorhombic
Space group	*I4/mmm*	*Pban*	*Pban*
a, Å	23.862(3)	13.7089(4)	26.3697(17)
b, Å	23.862(3)	26.6171(6)	13.4790(12)
c, Å	7.2102(14)	15.8127(4)	15.7382(6)
α (deg)	90.00	90.00	90.00
β(deg)	90.00	90.00	90.00
γ(deg)	90.00	90.00	90.00
V, $Å^3$	4105.5(11)	5769.9(3)	5593.9(7)
Z	2	4	4
ρ_{calc}/ mg mm^3	0.994	1.334	1.412
μ/mm^{-1}	1.105	1.517	1.569
collected/unique	3327/1079	14848/5093	16485/4935
GOF on F^2	1.175	1.105	1.150
R_1/wR_2 [$I > 2\sigma(I)$]	0.0648, 0.1859	0.0550,0.1521	0.1254, 0.3315
R_1/wR_2 (all data)	0.0705, 0.1957	0.0620,0.1569	0.1414, 0.3427
diff. peak/hole	1.92/-0.63	1.10/-0.49	1.63/-1.27